RSC Advances

COMMUNICATION

Cite this: *RSC Adv.*, 2016, **6**, 114779

Single-stranded structure of alginate and its conformation evolvement after an interaction with calcium ions as revealed by electron microscopy

Xiaoyan He,[ab] Yi Liu,[a] He Li[a] and Hua Li*[a]

Received 5th September 2016
Accepted 30th November 2016

DOI: 10.1039/c6ra22212a

www.rsc.org/advances

The single-stranded structure of alginate and its conformations of the egg-box junctions after binding with Ca^{2+} ions were visualized for the first time by electron microscopy. The exaggerated egg-box junctions of the calcium alginate assembly consisted of four repeating units, each of which comprised three Ca^{2+}-linked G-block pairs and one M-block pair.

Alginate is a linear polysaccharide composed from homopolymeric regions of β-D-mannuronate (M) or α-L-guluronate (G) residues connected by covalent bonds.[1,2] It has been established that alginate triggers the severe fouling of the membranes and coatings,[3] which is predominately due to the fact that the components of this extracellular polymer substance provides mechanical stability to the microbial biofilms and substantially decide the adhesion of the microorganisms on the solid surfaces.[4] To control the undesirable biofouling, it is essential to understand the structure of alginate and its adsorption behaviors. Like most ionic polysaccharides, alginate offers the capability to form bonds with metal ions by binding with the divalent cations to increase its structural integrity or mechanical strength.[5] It has been clarified that alginate can form bonds with most divalent cations and the binding affinities increase in the order of $Mg^{2+} \ll Mn^{2+} < Ca^{2+} < Sr^{2+} < Ba^{2+} < Cu^{2+} < Pb^{2+}$.[6,7] In the alginate chain, G-blocks are believed to combine with the divalent cations, allowing alginate to form gels. Moreover, MG blocks affect the flexibility of the polysaccharide chains and, therefore, tend to change the viscosity of the alginate solution. The unique gelling properties of alginate are vital for its severe fouling properties. Therefore, clarification of the gelling properties and mechanism describing the linking of alginate with the divalent cations, especially Ca^{2+}, is essential for understanding the alginate-associated fouling at the molecular level.

Pioneering studies performed in 1973 on the interactions between the polysaccharides and divalent cations suggested an egg-box hypothesis based on circular dichroism spectral analyses.[8] This model suggests that the cations may be burdened and coordinated in a corrugated egg-box by G sequences. Further structure examination of alginate was attempted using a variety of techniques, such as isothermal titration calorimetry (ITC),[1] fiber X-ray diffraction with small-angle X-ray scattering,[5] Raman microscopy,[9] and size-exclusion chromatography.[10] However, to the best of our knowledge, to date, the direct visualization of the polysaccharide after binding with the divalent metal ions has not been reported. Moreover, knowledge on the dynamic binding process of the single-stranded alginate with the divalent cations towards the formation of egg-box junctions is still lacking. The structural changes in the alginate chains after binding with calcium cations remains unknown.

Previously available morphological characterization of alginate was based on the simple observation of the polysaccharide.[11] In this study, we employed negative-staining electron microscopy (NS-EM) to visualize, for the first time, the single-stranded structure of alginate adsorbed on a graphene surface. EM observation of the biological molecules in a single particle form is a developing approach in the structural biology for the study of molecular assemblies, which is widely used in the protein structural analysis.[12] Herein, the compatible interaction between calcium alginate and an unexpectedly big egg-box structure was also revealed and elucidated.

Sodium alginate (Aladdin Industrial Corp., China) and other chemical reagents (Sinopharm Chemical Reagent Co. Ltd, China) were used as received without any further purification. Alginate was further characterized by nuclear magnetic resonance (NMR, 400 MHz AVANCE III, Switzerland) at 50 °C using D_2O as the solvent and DSS (sodium 2,2-dimethyl-2-silapentane-5-sulfonate) as an internal reference. Prior to characterization, alginate was hydrolyzed into fragments in a boiling water bath

[a]*Key Laboratory of Marine Materials and Related Technologies, Zhejiang Key Laboratory of Marine Materials and Protective Technologies, Ningbo Institute of Materials Technology and Engineering, Chinese Academy of Sciences, 315201, Ningbo, China. E-mail: lihua@nimte.ac.cn; Fax: +86-574-86685159; Tel: +86-574-86686224*

[b]*University of Chinese Academy of Sciences, 100049, Beijing, China*

for 1 h after its pH value was adjusted to 3 by adding 1 mol L^{-1} HCl. Then, the solution pH was adjusted to 7 by adding 1 mol L^{-1} NaOH. Subsequently, the solution was transferred to a dialysis bag (MWCO: 3500 Da, MD: 34 mm, Beijing Solarbio Technology Co. Ltd, China) for exhaustive dialysis against distilled water for 24 h to remove the free ions. The solution was then put into vacuum freezing dryer to obtain a powder for characterization. Calcium alginate was produced by mixing 1 mg mL^{-1} alginate solution with an equal volume of 1 mg mL^{-1} $CaCl_2$ solution. The mixed solution was dialyzed for 24 h to remove the free ions after a complete reaction. The solution was then placed into a vacuum freezing dryer to obtain a powder for further characterization. The powder was examined by Fourier-transform infrared spectroscopy (FTIR, Nicolet 6700, USA) detected with a resolution of 4 cm^{-1} and a scan range from 4000 to 400 cm^{-1}. Identical normalization was conducted for the acquired FTIR spectra.

The morphology of the polysaccharides was characterized by transmission electron microscope (TEM, FEI Tecnai F20, the Netherlands) operated at 200 kV. For acquiring the EM images, low-dose conditions (10–15 e $Å^{-2}$) were employed. The negatively stained samples were prepared using the drop by drop protocol.[13] Briefly, a 7 μL drop of graphene suspension in ethanol was placed onto a micro grid following the complete evaporation of the solvent, and then a 7 μL drop of the alginate solution (0.01 mg mL^{-1} alginate in deionized water) was applied on it. After incubating for 15 min at room temperature, the excess solution was removed by blotting with filter paper. Two consecutive drops of 7 μL 2% (w/v) uranyl acetate solution were then applied on the grid for staining. Excess stain was removed by blotting and the grid was quickly air dried at room temperature after final blotting. For TEM characterization of the calcium alginate samples, calcium-alginate was prepared in a solution containing 0.002 mg mL^{-1} alginate solution and 0.001 mg mL^{-1} $CaCl_2$. Excess ions were removed by dialysis.

The G/M composition of the alginate used in this research was examined by high-resolution ^{1}H-NMR (Fig. 1a). Based on the characterization, the monomeric (F_G, F_M), the diadic (the nearest neighbors F_{GG}, F_{GM}, F_{MG}, F_{MM}), and the G-centered triadic (the next-nearest neighbors F_{GGG}, F_{GGM}, F_{MGG}, F_{MGM}) fractions can be obtained by area integration. The distribution of M and G residues was measured by the parameter η, defined by $\eta = F_{MG}/(F_M \times F_G)$, to characterize the sequence distributions.[14] As $0 \leq \eta < 1$, consecutive G-block and consecutive M-block are the main blocks in alginate chain.[14] In this case, η was calculated to be ~0.50, indicating a linear structure for the polysaccharide used in this study. Further IR detection of alginate (Fig. 1b) reveals the typical peaks located at ~1030 cm^{-1}, which refer to the C–OH and C–O–C stretching modes of alginate.[15] The bands at 1610 cm^{-1} and 1416 cm^{-1} are attributed to the asymmetric stretching vibration and symmetric stretching vibration of the carboxylate anion, respectively.[16] As shown in Fig. 1b and tabulated in Table 1, after the linking of alginate with calcium ions, there are minor frequency shifts in the carbohydrate region, especially in the 1650–1020 cm^{-1} region, which has also been previously realized.[16] The peaks are downshifted from 1608.71, 1126.25, and 1094.95 cm^{-1} (in sodium alginate) to 1604.25, 1124.93, and 1085.64 cm^{-1} (in calcium alginate), respectively. The shift to lower frequencies is indicative of a weakening in the C=O and C–O bonds, most likely due to the possibility that these bonds are shared with calcium ions.[17] Replacement of sodium ions by calcium ions should also account for the peak shifting since the replacement results in a new environment around the carbonyl groups. The

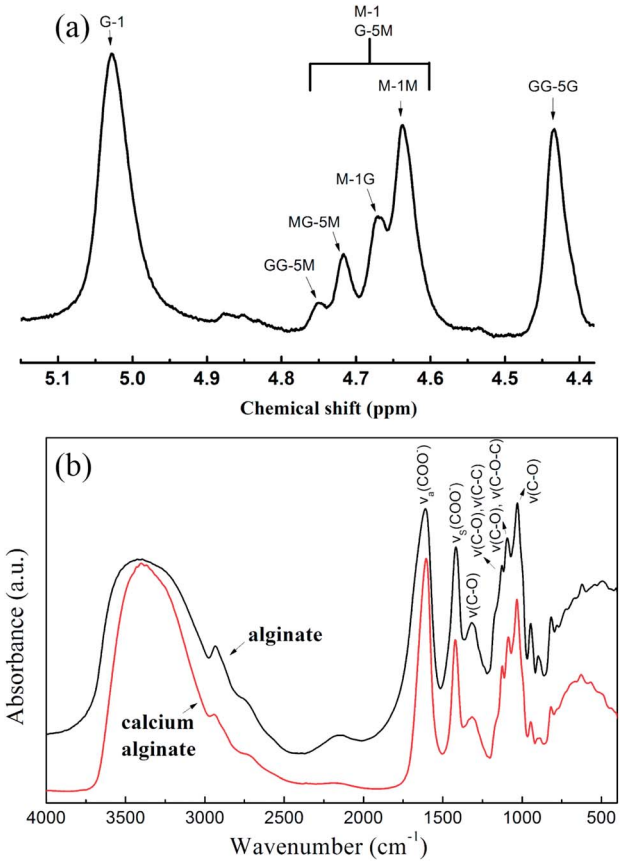

Fig. 1 Characterization of alginate: (a) ^{1}H-NMR spectrum (anomeric region) of alginate. M–1M and M–1G represent the anomeric proton of an M residue neighboring another M residue or a G residue. MG–5M, GG–5M, and MG–5G refer to the H-5 proton of the central G residue in an MGM, GGM, or MGG triad, respectively. G-1 is assigned to the anomeric proton of G residues and GG–5G refers to the anomeric proton of G residues in G-blocks. (b) IR spectra of alginate and calcium alginate. ν: stretching; s: symmetric; and a: asymmetric.

Table 1 Assignment of the IR adsorption bands for sodium alginate and calcium alginate[a]

Sodium alginate/(cm^{-1})	Calcium alginate/(cm^{-1})	Assignment
1608.71	1604.25	ν_a(COO$^-$)
1416.88	1420.97	ν_s(COO$^-$)
1317.56	1316.11	ν(C–O)
1126.25	1124.93	ν(C–O), ν(C–C)
1094.95	1085.64	ν(C–O), ν(C–O–C)
1028.45	1032.16	ν(C–O)

[a] ν: stretching; s: symmetric; a: asymmetric.

electron density around the carbonyl group is lowered when sodium ions are replaced by calcium ions due to the fact that the electron affinity of Ca^{2+} is much stronger than that of Na^{+}. The bond energy reduces with the decreasing wavenumber.[17] The IR spectra provides an evidence for the formation of insoluble calcium alginate after the mixing of $CaCl_2$ with soluble sodium alginate. Moreover, shifts in the FTIR bands of calcium alginate indicate complete cross-linking of alginate with calcium ions since no shift was observed in the FTIR bands for incomplete cross-linked calcium alginate.[18]

Further EM characterization reveals the rope-like morphology of the alginate adsorbed on the graphene surface (Fig. 2a-1). This is in good agreement with the NMR characterization that the polysaccharide used in this research has a linear structure. The width of the polysaccharide observed from the EM images is ~1 nm, a bit wider than the actual width of a single-chain of alginate. This is likely due to the cladding of the heavy metal stains used for the EM sample preparation. The EM structure further evidences the adsorbed polysaccharide to be a single alginate molecule. Statistical analysis based on the acquired EM images shows that majority of the adsorbed sodium alginate molecules have lengths ranging from 105 to 385 nm.

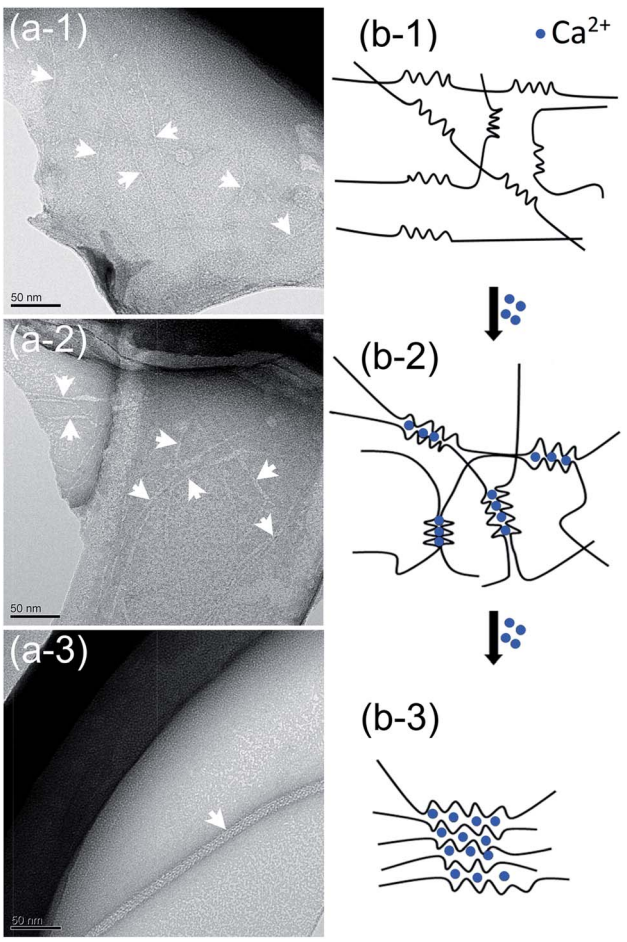

Fig. 2 EM images showing conformation evolvement of alginate molecules before (a-1) and after (a-2 and a-3) linking to calcium ions with increasing duration. The conformational changes are schematically depicted based on the egg-box model (b-1–b-3). The white arrows point to the typical molecules.

After linking with calcium ions, the structure of the alginate molecule significantly evolves (Fig. 2). To elucidate the binding process, EM images were acquired for the samples with different adsorption times. It is clear that the width of the alginate chain becomes bigger over time, showing good agreement with the multiple-step binding of Ca^{2+} to short-chain alginate.[1] Based on the previously proposed egg-box interaction model,[5,8] the evolved structures are schematically depicted in Fig. 2b. Although past extensive research efforts on alginate have been mainly involved in its ability to bind the divalent cations,[6,7] our study has clearly shown the structure of both alginate and calcium alginate molecules. At the very beginning, the width of the chain was ~1 nm (Fig. 2a-1), indicating the unlinking of calcium cations from alginate. Subsequently, the increase in the width to 3–5 nm (Fig. 2a-2) suggests the formation of an egg-box dimer by a few alginate chains with inside free calcium (Fig. 2b-2). Calcium ions are usually recruited by the electrostatic attraction.[1] Calcium alginate continues to grow by forming inter-clusters of multimers with a width of ~10 nm (Fig. 2a-3 and b-3).

Although the images have relatively low resolution due to the staining of heavy metals, the enlarged view clearly shows the morphological features of the calcium alginate multimer and provides clues for the binding regimes of Ca^{2+} with alginate fragments (Fig. 3). It is already established that one calcium ion electrostatically cross-links with the GG block of alginate, forming an egg-box structure.[19] Our EM characterization agrees well with this model. Surprisingly, it is noted that the linear length of the recognizable egg-box structure is ~4.3 nm (Fig. 3a), almost five times that of one junction zone of calcium alginate, ~0.87 nm.[5,20] Therefore, it is suggested that the calcium alginate molecules might be tangling together. To elucidate the conformational changes of alginate after linking with the divalent calcium ions, the atomic structure of the chains containing calcium ions[19] was docked into the enlarged 2D EM image (Fig. 3b and c). The preliminary docking was displayed in Chimera based on the position and size of the G-blocks.[21] The surface views of the atomic structure of Ca^{2+}-linked G-block and M-block pairs favorably fit with the backbone of the EM image (Fig. 3b). Strikingly, it is noted that for one backbone of the calcium alginate adsorbed on the surface of the materials, three G-block pairs together with one M-block pair and work as a repeating unit, two of which are interconnected by the M-block pairs (Fig. 3c and d). Our finding agrees very well with the speculations that an M-block usually accounts for the ability of the molecular chains to bend.[11] Herein, it seems clear that three egg-box domains and one M-block pair form a repeating unit, giving rise to the formation of a much bigger egg-box structure consisting of twelve small egg-box domains. The overall size (diameter) of the twisted structure is determined by the number of similar chains that are interconnected together. This has already been proven in this study that the continuous recruitment of calcium ions resulted in an increased size of the chains (Fig. 2). In addition, it is interesting to note that the "buckled" conformation leaves repeating unfilled caves. Our further

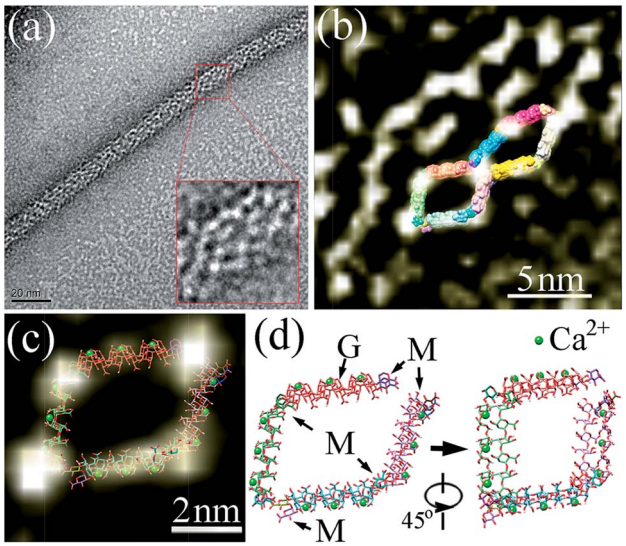

Fig. 3 Domain organization and negative-staining EM image analysis of the repeating calcium alginate unit. (a) The EM image shows calcium alginate assembly (inset is an enlarged view of the selected area used for further docking analyses). (b) The selected 2D image of the molecule in comparison with the surface view of the atomic structure of G–M residues. Preliminary docking was made into the repeating unit. The special alignment of the significantly enlarged individual egg-box results in a spiral conformation. (c) Enlarged view of one repeating unit shows that the repeating unit consists of three pairs of Ca^{2+}-linked G-blocks and one M-block pair. (d) Proposed model of the repeating unit derived from the negative-staining EM images (M: M-block, G: G-block).

ongoing efforts are devoted to clarifying and elucidating the 3D structures of the chains.

Conclusions

The single-strand morphology of alginate and the egg-box conformation of calcium alginate were obtained for the first time by negative-staining electron microscopy. This approach is effective for visualizing the structures of the polysaccharides adsorbed on the surfaces of materials and the interaction at different stages, providing relatively low-resolution structures of the complexes, but with an excellent contrast showing the structural feature of the molecules. Cross-linking of calcium ions altered the structural features of the alginate chains, thus achieving a stable tangling conformation with a special enlarged egg-box arrangement.

Acknowledgements

This research was supported by the National Natural Science Foundation of China (grant # 31271017, 41476064, and 51401232), the Project of Scientific Innovation Team of Ningbo (grant # 2015B11050), and the China Postdoctoral Science Foundation (grant # 2016T90554 and 2014M561800).

Notes and references

1 Y. Fang, S. Al-Assaf, G. O. Phillips, K. Nishinari, T. Funami, P. A. Williams and L. Li, *J. Phys. Chem. B*, 2007, **111**, 2456–2462.
2 S. L. Liu, J. Ling, K. W. Li, F. Yao, O. Oderinde, Z. H. Zhang and G. D. Fu, *RSC Adv.*, 2016, **6**, 63171–63177.
3 Q. L. Li, Z. H. Xu and I. Pinnau, *J. Membr. Sci.*, 2007, **290**, 173–181.
4 O. Orgad, Y. Oren, S. L. Walker and M. Herzberg, *Biofouling*, 2011, **27**, 787–798.
5 P. Sikorski, F. Mo, G. Skjåk-Bræk and B. T. Stokke, *Biomacromolecules*, 2007, **8**, 2098–2103.
6 T. Baumberger and O. Ronsin, *Biomacromolecules*, 2010, **11**, 1571–1578.
7 C. K. Siew, P. A. Williams and N. W. Young, *Biomacromolecules*, 2005, **6**, 963–969.
8 G. T. Grant, E. R. Morris, D. A. Rees, P. J. C. Smith and D. Thom, *FEBS Lett.*, 1973, **32**, 195–198.
9 N. P. Ivleva, M. Wagner, H. Horn, R. Niessner and C. Haisch, *Anal. Bioanal. Chem.*, 2009, **393**, 197–206.
10 I. M. N. Vold, K. A. Kristiansen and B. E. Christensen, *Biomacromolecules*, 2006, **7**, 2136–2146.
11 R. Gang, *J. Phys. Chem. Biophys.*, 2012, **2**, e103.
12 A. W. Decho, *Carbohydr. Res.*, 1999, **315**, 330–333.
13 H. Li, M. Chavan, H. Schindelin, W. J. Lennarz and H. Li, *Structure*, 2008, **16**, 432–440.
14 H. Grasdalen, B. Larsen and O. Smidsred, *Carbohydr. Res.*, 1979, **68**, 23–31.
15 P. Sundarrajan, P. Eswaran, A. Marimuthu, L. B. Subhadra and P. Kannaiyan, *Bull. Korean Chem. Soc.*, 2012, **33**, 3218–3224.
16 C. G. van Hoogmoed, H. J. Busscher and P. de Vos, *J. Biomed. Mater. Res., Part A*, 2003, **67**, 172–178.
17 B. S. Yeo, Z. H. Chen and W. S. Sim, *Langmuir*, 2003, **19**, 2787–2794.
18 S. Bekin, S. Sarmad, K. Gürkan, G. Yenici, G. Keçeli and G. Gürdağ, *Polym. Eng. Sci.*, 2014, **54**, 1372–1382.
19 I. Braccini, R. P. Grasso and S. Pérez, *Carbohydr. Res.*, 1999, **317**, 119–130.
20 E. E. Urena-Benavides and C. L. Kitchens, *Macromolecules*, 2011, **44**, 3478–3484.
21 E. F. Pettersen, T. D. Goddard, C. C. Huang, G. S. Couch, D. M. Greenblatt, E. C. Meng and T. E. Ferrin, *J. Comput. Chem.*, 2004, **25**, 1605–1612.